Published in final edited form as:
Circulation. 2011 September 13; 124(11 0): S18–S26. doi:10.1161/CIRCULATIONAHA.110.009431.

Computational Protein Design to Re-Engineer Stromal Cell-Derived Factor-1α (SDF) Generates an Effective and Translatable Angiogenic Polypeptide Analog

William Hiesinger, M.D.[1], **Jose Manuel Perez-Aguilar, B.S.**[2], **Pavan Atluri, M.D.**[1], **Nicole A. Marotta, B.S.**[1], **John R. Frederick, M.D.**[1], **J. Raymond Fitzpatrick III, M.D.**[1], **Ryan C. McCormick, B.S.**[1], **Jeffrey R. Muenzer, B.S.**[1], **Elaine C. Yang, B.S.**[1], **Rebecca D. Levit, M.D.**[3], **Li-Jun Yuan, M.D.**[4], **John W. MacArthur, M.D.**[1], **Jeffery G. Saven, Ph.D.**[2], and **Y. Joseph Woo, M.D.**[1]

[1]Division of Cardiovascular Surgery, Department of Surgery, University of Pennsylvania School of Medicine, Philadelphia, PA 19104

[2]Department of Chemistry, University of Pennsylvania School of Arts and Sciences, Philadelphia, PA 19104

[3]Division of Cardiology, Department of Medicine, Emory University School of Medicine, Atlanta, GA 30322

[4]Penn Cardiovascular Institute, University of Pennsylvania School of Medicine, Philadelphia, PA 19104

Abstract

BACKGROUND—After ischemic injury, cardiac secretion of the potent endothelial progenitor stem cell (EPC) chemokine SDF stimulates endogenous neovascularization and myocardial repair, a process insufficiently robust to repair major infarcts. Experimentally, exogenous administration of recombinant SDF enhances neovasculogenesis and cardiac function after MI. However, SDF has a short half-life, is bulky, and very expensive. Smaller analogs of SDF may provide translational advantages including enhanced stability and function, ease of synthesis, lower cost, and potential modulated delivery via engineered biomaterials. In this study, computational protein design was used to create a more efficient evolution of the native SDF protein.

METHODS and RESULTS—Protein structure model was used to engineer an SDF polypeptide analog (**ESA**) that splices the N-terminus (activation and binding) and C-terminus (extracellular stabilization) with a diproline segment designed to limit the conformational flexibility of the peptide backbone and retain the relative orientation of these segments observed in the native

Corresponding Author: Y. Joseph Woo, M.D. 3400 Spruce St. 6 Silverstein Philadelphia, PA 19104 Phone: 215-662-2956 Fax: 215-349-5798 wooy@uphs.upenn.edu.

Disclosures
None.

structure of SDF. EPCs in **ESA** gradient, assayed by Boyden chamber, showed significantly increased migration compared to both SDF and control gradients (**ESA** 567±74 cells/HPF vs SDF 438±46 p=0.037; vs Control 156±45 p=0.001). EPC receptor activation was evaluated by quantifying phosphorylated AKT. **ESA** had significantly greater pAKT levels than SDF and control (1.64±0.24 vs 1.26±0.187, p=0.01; vs. 0.95±0.08, p<0.001). Angiogenic growth factor assays revealed a distinct increase in Angiopoietin-1 expression in the **ESA** and SDF treated hearts. Also, CD-1 mice (n=30) underwent LAD ligation and peri-infarct intramyocardial injection of **ESA**, SDF-1α, or saline. At 2 weeks, echocardiography demonstrated a significant gain in EF, CO, SV, and Fractional Area Change (FAC) in mice treated with **ESA** when compared to controls and significant improvement in FAC when compared to SDF treated mice.

CONCLUSION—When compared to native SDF, a novel engineered SDF polypeptide analog (ESA) more efficiently induces EPC migration and improves post-MI cardiac function, and thus offers a more clinically translatable neovasculogenic therapy.

Keywords

Angiogenesis; Cardiac Surgery; Computer-Based Model; Coronary Microvascular Function; Endothelial Progenitor Cells

Background

More people die annually from cardiovascular disease than from any other cause. The World Health Organization estimates that more than 17 million people per year die from cardiovascular disease. Of these deaths, an estimated 7.2 million were due to ischemic heart disease. An estimated 80,000,000 American adults (approximately 1 in 3) have at least one type of cardiovascular disease with more than 22,000,000 suffering from either coronary heart disease or heart failure.[1]

Treatments for ischemic heart disease often fail because they do not address the underlying ventricular cellular pathophysiology and, most importantly, do not restore microvascular perfusion, which has been shown to be a critical, independent predictor of ventricular remodeling as well as reinfarction, heart failure, and death.[2,3] On the other hand, post-infarction patients who develop robust angiographic collateralization manifest improved regional ventricular function, suggesting an important role of the native revascularization process.[4] Current therapeutic options for ischemic heart disease are only capable of intervening in relatively large arteries, leaving pervasive microvascular dysfunction unaddressed. This is important because microvascular integrity, specifically microvascular blood velocity and flow, predicts functional recovery of ischemic myocardium.[5-9] In addition, current interventions are instituted relatively late in the overall timecourse of the disease process with macrorevascularization possible in only 63–80% of patients with ischemic heart disease.[10] Even with re-establishment of epicardial coronary artery flow through thrombolysis, percutaneous intervention, or bypass grafting, a paucity of patent, functional microvasculature remains. Angiogenic cytokine therapy is a microrevascularization strategy that can serve as a primary therapy at any point in the disease process and can be employed synergistically with traditional coronary

revascularization methods.[11] A wide variety of cytokines and microrevascularization techniques have been employed with varying degrees of success.[12-15]

Stromal cell-derived factor-1α (SDF) is a powerful chemoattractant and considered to be one of the key regulators of hematopoietic stem cell trafficking between the peripheral circulation and bone marrow. It has been shown to effect EPC proliferation and mobilization to induce vasculogenesis, and is significantly upregulated in response to both myocardial ischemia and infarction.[16, 17] SDF, a 67 amino acid protein, is also remarkably conserved among species; a single amino acid substitution is all that differentiates the human and murine sequences.[18] Experimentally, delivery of SDF to ischemic myocardium has been shown to increase circulating EPCs, significantly enhance myocardial endothelial progenitor cell density, increase vasculogenesis, and augment myocardial function by enhancing perfusion, reversing cellular ischemia, increasing cardiomyocyte viability, and preserving ventricular geometry.[19, 20]

However, recombinant SDF is quickly degraded by multiple proteases[18, 21], has a large and complex tertiary structure involving multiple disulfide linkages[22], and is very expensive since it is a recombinant protein. Smaller analogs of SDF may provide translational advantages including enhanced stability and function, ease of synthesis, lower cost, and potential modulated delivery via engineered biomaterials.[23, 24] In the present study, we set out to design and engineer a minimized highly efficient polypeptide analog of the SDF molecule using computational molecular modeling and design. The primary design goal was to remove the large, central β-sheet region and link the native N-terminus (responsible for receptor activation and binding) and the C-terminus (responsible for extracellular stabilization) while maintaining functionality and the approximately perpendicular orientation between the two termini.[22] Two disulfide bonds located in the large central β-sheet region help to maintain the conformation of native SDF. In order to recover a similar conformation after excision of this portion of the protein, proline residue linkers were considered to connect the N- and C-termini. The cyclic proline residue limits the conformational space accessible to the polypeptide. Loop modeling calculations revealed the variability of conformations explored by linkers comprising different numbers of proline residues. A designed diproline linker yielded energetic and conformational advantages resulting in a small, low molecular weight engineered SDF polypeptide analog (ESA) that was shown to have activity comparable to or better than recombinant human SDF both in vitro and in a murine model of ischemic heart failure.

Methods

Computational Protein Design, Modeling, and Synthesis

Loop modeling calculations were carried out using the program MODELLER, which implements a loop modeling algorithm that consists of an optimization of a defined segment of protein structure in a fixed environment, guided by a pseudo energy scoring function.[25] Fifty different structures for a one, two, and three proline residue linker were created while constraining the coordinates of the remainder of the protein. The conformation with the lowest effective energy (best score) was analyzed using Molprobity, which provides detailed all-atom contact analysis of steric interactions, dihedral angles, and possible hydrogen bonds

and van der Waals contacts.[26] After the amino acid sequence of the newly designed ESA peptide had been computationally designed and analyzed, it was synthesized utilizing solid phase peptide synthesis which involves the incorporation of N-a-amino acids into a peptide of any desired sequence with one end of the sequence remaining attached to a solid support matrix. After the desired sequence of amino acids has been obtained, the peptide is removed from the polymeric support.

Cell Isolation

Bone marrow mononuclear cells (MNC) were isolated from the long bones of adult male Green Fluorescent Protein (GFP)-Wistar rats by density-gradient centrifugation with Histopaque 1083 (Sigma) and cultured in Endothelial Basal Medium-2 supplemented with EGM-2 Singlequot (Lonza) containing hEGF, FBS, VEGF, hFGF-B, R3-IGF-1, ascorbic acid, heparin, gentamicin, and amphotericin-B. The combination of endothelial specific media and the removal of nonadherent MNCs was intended to select for the EPC phenotype.

Functional Characterization of Isolated EPCs by Boyden Chamber Assay

Boyden chambers (Neuro Probe) were employed to assess EPC migration. Briefly, 8 μm filters were loaded into control and experimental chambers. Fourteen day EPCs cultured in endothelial specific media on vitronectin coated plates were trypsinized, counted, and brought to a concentration of 90cells/μl in Dulbecco's phosphate buffered saline (DPBS). The bottom chamber of the control and experimental chambers were loaded with DPBS, 100ng/ml recombinant SDF (R&D systems) in DPBS, or 100ng/ml ESA in DPBS. A 560μl cell suspension was added to the top chamber of each. All three chambers were incubated at 37°C, 5%CO_2 for 4 hours. The cells remaining in the top chamber were wiped clean with a cotton swab and the filter was removed. Slides were visualized on a DF5000B Leica Fluorescent scope and analyzed via LASAF version 2.0.2 (Leica) software. Boyden chamber analysis was performed in triplicate. Additional Boyden Chamber assays were run to generate a dose/response curve comparing molar equivalents of ESA and SDF. A series of progressively increasing ESA and SDF gradients (0.625nM, 1.25nM, 2.5nM, 5nM, 12.5nM, 20nM, 25nM, and 50nM) were utilized and assays at each dose were run ten times.

CXCR4 Receptor Activation Assay

Fourteen day EPCs cultured in endothelial specific media on vitronectin coated plates were trypsinized and plated onto the bottom of a 96-well cell culture plate at a density of 10,000 cells per well and allowed to adhere for 24hrs. Cells were incubated with culture media containing recombinant SDF (0.5ug/mL) or ESA (0.5ug/mL) or media only (control) for 10 minutes and subsequently fixed in 4% formaldehyde. Phosphorylated and total AKT levels were quantified using FACE AKT ELISA Kit (Active Motif). These experiments were also repeated out with the addition of the CXCR4 receptor antagonist AMD3100 to each experimental group. Results are reported in optical density (OD) units.

CXCR4 Receptor Expression

EPCs were seeded overnight at a density of 1×10^4 cells per cover slip in four well slide chambers. Cells were either treated with 100 ng/ml SDF or 100 ng/ml ESA at 37°C for six

hours. Following chemokine stimulation, the cells were fixed and immunostained with rabbit anti-CXCR4 antibody (Abcam) at 1:250 for 12 hours. Cells were then incubated with Alexa 488 donkey anti-rabbit polyclonal antibody (Invitrogen) at 1:250 for one hour at room temperature. The cells were counterstained with DAPI to visualize nuclei. The immunofluorescence images were acquired using Zeiss ZEN 2010 software and a Zeiss LSM 710 confocal laser fluorescence scanning microscope.

Animal Care and Biosafety

Male CD-1 mice weighing 25 - 30 g were obtained from Charles River. Food and water were provided ad lib. This investigation conforms with the *Guide for the Care and Use of Laboratory Animals* published by the US National Institutes of Health (NIH Publication No. 85-23, revised 1996) and was approved by the Institutional Animal Use and Care Committee of the University of Pennsylvania (Protocol #709026).

Ischemic Cardiomyopathy Model

Mice were anesthetized with ketamine (100 mg/kg) and xylazine (10 mg/kg), intubated with a 22-gauge catheter, and mechanically ventilated (Hallowell EMC). With the animal supine, an anterior thoracotomy was performed in the left fourth intercostal space, and an 8-0 polypropylene suture was placed around the mid-left anterior descending coronary artery (LAD) midway between the left atrial appendage and left ventricular apex and ligated to produce a large anterolateral myocardial infarction of 30% of the left ventricle. The extent of infarction is highly reproducible in our hands and progression to cardiomyopathy has been well documented. Following ligation, animals were randomly assigned to receive direct intramyocardial injection into the peri-infarct borderzone of either saline (30 μl, n=7), SDF (6μg/kg in 30 μl, n=13), or ESA (6μg/kg in 30 μl, n=10). The thoracotomy was then closed and the animals were extubated and recovered. Buprenorphine (0.5mg/kg) was administered for postoperative analgesia. Both treatment groups received subcutaneous injections of 40 μg/kg liquid sargramostim (GMCSF), diluted in saline for a total volume of 100 l immediately postoperatively and on postoperative day one.

In Vivo Angiogenic Growth Factor Expression

To assess upregulation of angiogenic growth factors and evaluate any potential sustained angiogenic effect of ESA treatment, hearts from all animals (Control n=7, SDF n=13, and ESA n=10) were explanted two weeks following LAD ligation, and myocardial tissue biopsies were taken from the ischemic borderzone. Samples were homogenized in T-Per Tissue Extraction Reagent (Thermo-Fischer), normalized for total protein content via Quick Start Bradford Protein Assay (Bio-Rad Laboratories), and tested for presence of mouse Angiopoietin-1. Immunoblotting was performed using a mouse monoclonal antibody directed against mouse Angiopoietin-1 (1:250, Abcam), and Horseradish peroxidase conjugated sheep anti-mouse IgG ECL secondary antibody (1:20,000, GE Healthcare). Chemiluminescent SuperSignal West Dura Extended Duration Substrate (Thermo Scientific) was used and images were captured using a ChemiDoc XRS+ system (Bio Rad). Assays were performed in triplicate.

In Vivo Inflammatory Analysis

To assess upregulation of inflammatory factors, hearts from all animals (Control n=7, SDF n=13, ESA n=10) were explanted two weeks following LAD ligation, and myocardial tissue biopsies were taken from the ischemic borderzone. Samples were homogenized in T-Per Tissue Extraction Reagent (Thermo-Fischer), normalized for total protein content via Quick Start Bradford Protein Assay (Bio-Rad Laboratories), and tested for presence of mouse tumor necrosis factor alpha (TNFα). Immunoblotting was performed using a rabbit polyclonal antibody directed against mouse TNFα (1:1000, Abcam), and Horseradish peroxidase conjugated sheep anti-rabbit IgG ECL secondary antibody (1:3000, GE Healthcare). Chemiluminescent SuperSignal West Dura Extended Duration Substrate (Thermo Scientific) was used and images were captured using a ChemiDoc XRS+ system (Bio Rad).

To further assess the inflammatory response following treatment, hearts from a subset of animals (control, n=4; SDF, n=4; ESA, n=4) were explanted two weeks after LAD ligation, and myocardial tissue biopsies were taken from the ischemic borderzone. Samples were homogenized in T-Per Tissue Extraction Reagent (Thermo-Fischer), normalized for total protein content via Quick Start Bradford Protein Assay (Bio-Rad Laboratories), and tested for presence of multiple inflammatory markers including MCP-1, SCF, NF-κB, phospho-NF-κB, phospho-p38 MAPK, phospho-Stat3, and phospho-IκB-α. Levels were quantified using the Mouse Inflammation ELISA Strip (Signosis, Sunnyvale) and the PathScan Inflammation Multi-Target Sandwich ELISA (Cell signaling Technology, Danvers).

Echocardiographic Assessment of LV Geometry and Function

Left ventricular (LV) geometry and function were evaluated at 2 weeks (Control n=7, SDF n=13, ESA n=10) following LAD ligation using a high-resolution (30 MHz) Vevo 770 transthoracic echocardiography system (VisualSonic Inc., Toronto, Canada). Four-equally-spaced short-axis and one maximum long-axis cine-loop acquisitions of the left ventricle (LV) were recorded with ultrahigh-frame-rate EKVTM (ECG-based kilohertz visualization) acquisition mode. The LV systolic function was evaluated by modified 4-plane Simpson's method. LV cross-sectional areas were obtained by tracing the diastolic and systolic endocardial borders in each of the four equally-spaced LV short-axis slices. Based on these measurements and the Simpson Length (d, s), the fractional area change (FAC, %), ejection fraction (EF, %), stroke volume (SV, ul) and cardiac output (CO, ml) were computed using the Vevo 770 Standard Measurement Package. Before and during the ultrasound scanning, the mouse was lightly anesthetized with a mixture of 1-2% Isoflurane gas and 100% oxygen, and was placed in the supine position on a heating platform.All analyses were performed by a single investigator in a group blinded fashion.

Statistical Analysis

Overall comparisons between the three groups were analyzed using a oneway analysis of variance (ANOVA). The results are reported using F (a ratio of the variance between groups to the variance within groups), two degrees of freedom, and the p-value. In addition, the unpaired Student's t-test was used to compare individual groups. Values are expressed as mean ± standard error of the mean (SEM). Statistical significance was defined by $P \leq 0.05$.

Results

Computational Protein Design, Modeling, and Synthesis

The crystallographic structure of SDF at 2.2 Å resolution was used to guide design and modeling (Figure 1).[27] The central beta sheet region residues (amino acids 18-54) were replaced with a two-proline linker, resulting in the 32-residue designed polypeptide ESA. The coordinates of residues 14FESHPPL20 were allowed to relax upon modeling with MODELLER while the coordinates of the remainder of the structure were constrained at their crystallographic values. Fifty different possible structures were generated for peptides with a one, two, or three proline linker. In general, the number of stable conformations increases substantially as the number of linking amino acids is increased (Figure 2). The peptide with the two proline linker (subsequently designated ESA) yielded energetic and conformational advantages. The ESA peptide structure model with the lowest scoring function was chosen for further analysis. Importantly, the two proline residues were found to have energetically favorable backbone dihedral angles (ϕ and ψ) consistent with those observed for proline in natural protein structures (Figure 3). The introduction of a two consecutive proline linker does not produce steric clashes within the modeled polypeptide structure. In addition, based on the calculated structure, phenylalanine 14 ($F14^{ESA}$) is interacting with glutamic acid 15 ($E15^{ESA}$), histidine 17 ($H17^{ESA}$) and leucine 20 ($L20^{ESA}$ or L55 in SDF). These interactions are not present in the crystallographic structure of SDF and this group of residues may form a small cluster-like structure which, when coupled with the diproline spacer, bias the peptide toward conformations similar to those found in native SDF (Figure 4). Further structural analysis reveals that the model doesn't contain any steric clashes or unusual conformations of the backbone and the amino acid side chains.

EPCs Cultured in Endothelial Specific Media Exhibit Enhanced Migration When Exposed to an ESA gradient

Utilizing a Boyden chamber assay, 14 day cells show increased migration when placed in an ESA gradient when compared to both recombinant SDF and saline (ESA 567±74 cells/HPF vs. SDF 438±46, p=0.037 cells/HPF; vs. control 156±45 cells/HPF, p=0.001). Representative slides are shown in Figure 5. In addition, a one-way ANOVA was used to generate an overall comparison of the three study groups. EPC migration differed significantly across the three groups, $F(2, 6) = 41.27$, $p = 0.0003$. A dose response curve generated by comparing molar equivalents of ESA and SDF (Figure 6) demonstrated that ESA significantly outperforms SDF at the high end of the concentration range but was essentially equivalent to SDF for the low and mid range concentrations. Additionally, it was revealed that the effectiveness of ESA and SDF are not linearly correlated to the dose concentration and that there is a significant decrease in EPC migration at the very highest doses for both.

ESA Elicits Increased CXCR4 Receptor Activation In Vitro

Cells treated with ESA had greater levels of AKT phosphorylation than both recombinant SDF (1.638 ± 0.239 OD vs. 1.258 ± 0.187 OD, p=0.006) and control (1.638 ± 0.239 OD vs. 0.949 ± 0.077 OD, p=0.0003). There was no significant difference in total AKT content across all groups. In addition, a one-way ANOVA was used to generate an overall

comparison of the three study groups. Levels of AKT phosphorylation differed significantly across the three groups, $F(2, 21) = 38.56$, $p < 1 \times 10^{-7}$. The addition of the CXCR4 receptor antagonist AMD3100 to the culture media eliminated any difference in receptor activation between the groups (ESA 0.598 ± 0.22 OD vs. SDF 0.599 ± 0.07 OD, p=0.49 and ESA 0.598 ± 0.22 OD vs. Control 0.539 ± 0.05 OD, p=0.27).

EPCs Display Robust CXCR4 Expression When Treated With ESA

Following exposure to ESA or SDF for six hours, isolated EPCs demonstrate diffuse expression of the CXCR4 receptor (Figure 7).

In vivo Angiogenic Growth Factors Are Upregulated by ESA

At two weeks, immunoblotting revealed a significant quantitative increase in mouse Angiopoietin-1 expression in the ESA and SDF treated animals compared to the control group. Quantitative analysis demonstrated intensities of 336 ± 9 (ESA), 367 ± 17 (SDF), and 234 ± 7 (control) intensity units, respectively ($p<0.001$). A representative immunoblot is shown in Figure 8.

In vivo Levels of Borderzone Inflamatory Markers Are Not Statistically Different between Groups

At two weeks, immunoblotting revealed similar levels of TNFα between the ESA, SDF, and control groups. Quantitative analysis demonstrated intensities of 4784 ± 274 (ESA), 4832 ± 547 (SDF), and 4832 ± 722 (control) arbitrary intensity units, respectively. Statistical comparisons revealed no statistically significant difference (ESA vs. control, p=0.46; ESA vs. SDF, p=0.4, SDF vs. control, p=0.5). Additional analysis demonstrates that, following infarction and treatment, borderzone levels of the inflammatory factors MCP-1, SCF, NF-κB, phospho-NF-κB, phospho-p38 MAPK, phospho-Stat3, and phospho-IκB-α are either NOT significantly different or significantly less in animals treated with ESA or SDF when compared to saline control animals. These findings indicate that inflammation is not responsible for the beneficial and pro-angiogenic effects of ESA.

Echocardiographic Assessment Demonstrates Enhanced LV Function Following ESA Treatment

Echocardiographic assessment of cardiac function demonstrated significant benefits in the ESA group compared to the control group. At two weeks, ESA animals had a significantly improved ejection fraction (57 ± 2.9% vs. 42 ± 1.6%, p=0.002), cardiac output (30 ± 1.8 ml/min vs. 23 ± 1.3 ml/min, p=0.01), stroke volume (61 ± 3.6μl vs. 48 ± 2.9μl, p=0.02), and fractional area change (52 ± 3.6% vs. 29 ± 4.9%, p=0.001) when compared to controls. The ESA treated mice also had a significantly increased fractional area change when compared to SDF treated mice (52 ± 3.6% vs. 42 ± 3.2%, p=0.04) and a strong trend towards improvement in all other ventricular function parameters assessed [See Table 1]. A one-way ANOVA was used to generate an overall comparison of the three study groups for each cardiac functional parameter. Values differed significantly across the three groups for ejection fraction ($F(2, 27) = 5.71$, $p = 0.009$), cardiac output ($F(2, 27) = 3.98$, $p = 0.03$),

stroke volume (F (2, 27) = 3.83, p = 0.03), and fractional area change (F (2, 27) = 7.91, p = 0.002).

Discussion

Angiogenic cytokine therapy for ischemic heart disease has proven to have great potential in numerous pre-clinical and clinical trials. The ability to replenish myocardial microvasculature could prove life saving to the millions of patients with myocardial ischemia. SDF, in particular, is among the most potent and specific angiogenic cytokines; its sole target, the CXCR4 cell surface antigen, is expressed in significant levels on CD34+ EPCs and expression of this receptor is related to efficient SDF induced transendothelial migration.[28] SDF has been shown repeatedly to play a critical role in the rescue of myocardial function and stem cell recruitment to the heart after myocardial infarction.[19, 20, 29-33] However, significant barriers remain between the diverse experimental success of SDF angiogenic cytokine therapy and its wide spread clinical translation. SDF is a large, complex 10 kD protein that is expensive to manufacture and readily inactivated by proteases that are upregulated at the time of myocardial infarction.[34, 35] It is our belief that smaller, synthetic analogs of SDF can provide translational advantages over the native protein including enhanced stability and function, ease of synthesis, lower cost, and potential modulated delivery via engineered biomaterials. In this study, we employed advanced computational protein design techniques to create a more efficient and translatable molecule (ESA) evolved from the native SDF protein.

The ESA peptide was engineered to link the native N-terminus (responsible for receptor activation and binding) and the C-terminus (responsible for extracellular stabilization) with a diproline amino acid spacer. Though ESA may not have a well-defined tertiary structure, the linker is designed to bias the polypeptide toward structures that present the N- and C-termini in a manner similar to that present in the native SDF protein. Based on the modeled structure, $F14^{ESA}$ is in proximity to $E15^{ESA}$, $H17^{ESA}$ and $L20^{ESA}$ forming a small cluster of side chains within ESA (Figure 4). These interactions, coupled with the diproline linker, may provide a conformational bias sufficient to recover the activity associated with SDF. The end product, ESA, is a novel polypeptide that contains less than half of the number of amino acid residues, is less than half of the molecular weight, and has enhanced physiologic performance when compared to recombinant SDF.

The SDF chemotactic homing mechanism is central to its ability to increase peri-infarct microvasculature and prevent mechanically inefficient ventricular contraction and eventually heart failure. Utilizing a Boyden Chamber assay to directly quantify the magnitude of cellular migration, we were able to demonstrate significantly enhanced migration of endothelial progenitor stem cells when placed in an ESA gradient compared to native SDF peptide. This result shows that for the same mass concentration, ESA not only retains this important function, despite its reengineered conformation, but surpasses the native protein. Compared to SDF, the relatively small size of ESA may enhance its diffusion potential and the speed at which the chemotactic signal is deployed. However, rapid diffusion is likely not the only factor that leads to significantly greater EPC migration. It has been shown that AKT activation is required for SDF induced cellular migration.[36] To

evaluate the EPC response to ESA, we incubated EPCs with culture media containing ESA, recombinant SDF, or media only (control) and quantified both phosphorylated and total AKT levels by ELISA. In concordance with the results of the EPC migration assay, we were able to demonstrate significantly increased CXCR4 receptor activation and phosphorylated AKT levels in response to ESA when compared to SDF. Also, the addition of the CXCR4 antagonist AMD3100 eliminates this difference in receptor activation between ESA, SDF, and control, confirming receptor specificity. It is difficult to speculate which specific receptor-peptide interactions are responsible for the enhanced activation of CXCR4 by ESA and future computational studies will be employed to understand the surprisingly efficient activity of this novel polypeptide on a molecular level.

It is our belief that ESA, in a similar fashion to SDF, increases borderzone microvasculature which, in turn, reverses cellular ischemia, preserves cardiomyocyte viability, and increases the mechanical efficiency of peri-infarct myocardium. In support of that hypothesis, we have shown that borderzone myocardium treated with ESA has significantly upregulated levels of Angiopoietin-1, indicative of an ongoing angiogenic process as late as two weeks after infarction and treatment. One could argue that the mechanism responsible for the upregulated angiogenic activity is an exaggerated inflammatory response resulting from the injection of ESA or even SDF. However, analysis of borderzone TNFα, MCP-1, SCF, NF-κB, phospho-NF-κB, phospho-p38 MAPK, phospho-Stat3, and phospho-IκB-α, revealed that levels of inflammatory markers are not increased in experimental animals compared to controls indicating that the beneficial angiogenic and functional effects are not the result of differing levels of inflammation.

An increase in microvascular perfusion should result in decreased ventricular remodeling, improved regional ventricular function, and slower progression toward heart failure. Left ventricular geometry and function were evaluated at 2 weeks following LAD ligation using a high-resolution (30 MHz) transthoracic echocardiography system. The improved functionality of ESA in vitro was, once again, borne out in vivo. Animals treated with intramyocardial injections of the ESA peptide had better ejection fractions, cardiac output, stroke volume, and fractional area contraction than both the SDF and control groups.

In conclusion, we have been able to engineer a novel, low molecular weight polypeptide with the enhanced physiologic ability to induce EPC migration, EPC receptor activation, and improve ventricular performance when compared to native SDF. This peptide offers a more clinically translatable neovasculogenic therapy that could conceivably be deployed at any point in the time course of ischemic heart disease to address critical deficits in microvascular perfusion.

Acknowledgments

Sources of Funding

1. NIH 1R01HL089315-01 “Angiogenic Tissue Engineering to Limit Post-Infarction Ventricular Remodeling.” (YJW)
2. NIH NHLBI/Thoracic Surgery Foundation for Research and Education jointly sponsored Mentored Clinical Scientist Development Award, 1K08HL072812, “Angiogenesis and Cardiac Growth as Heart Failure Therapy.” (YJW)

3. The Thoracic Surgery Foundation Research Award (TSFRE). (WH)

4. NIH Training Grant, T32-HL-007843-13. “Training Program in Cardiovascular Biology and Medicine.” (WH)

5. National Science Foundation MRSEC DMR05-20020. (JGS)

References

1. Lloyd-Jones D, Adams R, Carnethon M, De Simone G, Ferguson TB, Flegal K, Ford E, Furie K, Go A, Greenlund K, Haase N, Hailpern S, Ho M, Howard V, Kissela B, Kittner S, Lackland D, Lisabeth L, Marelli A, McDermott M, Meigs J, Mozaffarian D, Nichol G, O'Donnell C, Roger V, Rosamond W, Sacco R, Sorlie P, Stafford R, Steinberger J, Thom T, Wasserthiel-Smoller S, Wong N, Wylie-Rosett J, Hong Y. Heart disease and stroke statistics--2009 update: a report from the American Heart 18 Association Statistics Committee and Stroke Statistics Subcommittee. Circulation. 2009; 119(3):e21–181. [PubMed: 19075105]

2. Araszkiewicz A, Grajek S, Lesiak M, Prech M, Pyda M, Janus M, Cieslinski A. Effect of impaired myocardial reperfusion on left ventricular remodeling in patients with anterior wall acute myocardial infarction treated with primary coronary intervention. Am J Cardiol. 2006; 98(6):725–728. [PubMed: 16950171]

3. Bolognese L, Carrabba N, Parodi G, Santoro GM, Buonamici P, Cerisano G, Antoniucci D. Impact of microvascular dysfunction on left ventricular remodeling and long-term clinical outcome after primary coronary angioplasty for acute myocardial infarction. Circulation. 2004; 109(9):1121–1126. [PubMed: 14967718]

4. Ejiri M, Fujita M, Sakai O, Miwa K, Asanoi H, Sasayama S. Development of collateral circulation after acute myocardial infarction: its role in preserving left ventricular function. J Cardiol. 1990; 20(1):31–37. [PubMed: 2093759]

5. Balcells E, Powers ER, Lepper W, Belcik T, Wei K, Ragosta M, Samady H, Lindner JR. Detection of myocardial viability by contrast echocardiography in acute infarction predicts recovery of resting function and contractile reserve. J Am Coll Cardiol. 2003; 41(5):827–833. [PubMed: 12628729]

6. Bolognese L, Cerisano G, Buonamici P, Santini A, Santoro GM, Antoniucci D, Fazzini PF. Influence of infarct-zone viability on left ventricular remodeling after acute myocardial infarction. Circulation. 1997; 96(10):3353–3359. [PubMed: 9396427]

7. Garot P, Pascal O, Simon M, Monin JL, Teiger E, Garot J, Gueret P, Dubois-Rande JL. Impact of microvascular integrity and local viability on left ventricular remodelling after reperfused acute myocardial infarction. Heart. 2003; 89(4):393–397. [PubMed: 12639866]

8. Rigo F, Varga Z, Di Pede F, Grassi G, Turiano G, Zuin G, Coli U, Raviele A, Picano E. Early assessment of coronary flow reserve by transthoracic Doppler echocardiography predicts late remodeling in reperfused anterior myocardial infarction. J Am Soc Echocardiogr. 2004; 17(7):750–755. [PubMed: 15220900]

9. Shimoni S, Frangogiannis NG, Aggeli CJ, Shan K, Quinones MA, Espada R, Letsou GV, Lawrie GM, Winters WL, Reardon MJ, Zoghbi WA. Microvascular structural correlates of myocardial contrast echocardiography in patients with coronary artery disease and left ventricular dysfunction: implications for the assessment of myocardial hibernation. Circulation. 2002; 106(8):950–956. [PubMed: 12186799]

10. Boodhwani M, Sodha NR, Laham RJ, Sellke FW. The future of therapeutic myocardial angiogenesis. Shock. 2006; 26(4):332–341. [PubMed: 16980878]

11. Atluri P, Woo YJ. Pro-angiogenic cytokines as cardiovascular therapeutics: assessing the potential. BioDrugs. 2008; 22(4):209–222. [PubMed: 18611064]

12. Atluri P, Panlilio CM, Liao GP, Suarez EE, McCormick RC, Hiesinger W, Cohen JE, Smith MJ, Patel AB, Feng W, Woo YJ. Transmyocardial revascularization to enhance myocardial vasculogenesis and hemodynamic function. J Thorac Cardiovasc Surg. 2008; 135(2):283–291. 291, e281. discussion 291. [PubMed: 18242252]

13. Jayasankar V, Woo YJ, Bish LT, Pirolli TJ, Chatterjee S, Berry MF, Burdick J, Gardner TJ, Sweeney HL. Gene transfer of hepatocyte growth factor attenuates postinfarction heart failure. Circulation. 2003; 108(Suppl 1):II230–236. [PubMed: 12970238]

14. Jayasankar V, Woo YJ, Pirolli TJ, Bish LT, Berry MF, Burdick J, Gardner TJ, Sweeney HL. Induction of angiogenesis and inhibition of apoptosis by hepatocyte growth factor effectively treats postischemic heart failure. J Card Surg. 2005; 20(1):93–9101. [PubMed: 15673421]
15. Kolakowski S, Berry MF, Atluri P, Grand T, Fisher O, Moise MA, Cohen J, Hsu V, Woo YJ. Placental growth factor provides a novel local angiogenic therapy for ischemic cardiomyopathy. J Card Surg. 2006; 21(6):559–564. [PubMed: 17073953]
16. Pillarisetti K, Gupta SK. Cloning and relative expression analysis of rat stromal cell derived factor-1 (SDF-1)1: SDF-1 alpha mRNA is selectively induced in rat model of myocardial infarction. Inflammation. 2001; 25(5):293–300. [PubMed: 11820456]
17. Yamaguchi J, Kusano KF, Masuo O, Kawamoto A, Silver M, Murasawa S, Bosch-Marce M, Masuda H, Losordo DW, Isner JM, Asahara T. Stromal cell-derived factor-1 effects on ex vivo expanded endothelial progenitor cell recruitment for ischemic neovascularization. Circulation. 2003; 107(9):1322–1328. [PubMed: 12628955]
18. De La Luz Sierra M, Yang F, Narazaki M, Salvucci O, Davis D, Yarchoan R, Zhang HH, Fales H, Tosato G. Differential processing of stromal-derived factor-1alpha and stromal-derived factor-1beta explains functional diversity. Blood. 2004; 103(7):2452–2459. [PubMed: 14525775]
19. Atluri P, Liao GP, Panlilio CM, Hsu VM, Leskowitz MJ, Morine KJ, Cohen JE, Berry MF, Suarez EE, Murphy DA, Lee WMF, Gardner TJ, Sweeney HL, Woo YJ. Neovasculogenic therapy to augment perfusion and preserve viability in ischemic cardiomyopathy. Ann Thorac Surg. 2006; 81(5):1728–1736. [PubMed: 16631663]
20. Woo YJ, Grand TJ, Berry MF, Atluri P, Moise MA, Hsu VM, Cohen J, Fisher O, Burdick J, Taylor M, Zentko S, Liao G, Smith M, Kolakowski S, Jayasankar V, Gardner TJ, Sweeney HL. Stromal cellderived factor and granulocyte-monocyte colony-stimulating factor form a combined neovasculogenic therapy for ischemic cardiomyopathy. J Thorac Cardiovasc Surg. 2005; 130(2): 321–329. [PubMed: 16077394]
21. Davis DA, Singer KE, De La Luz Sierra M, Narazaki M, Yang F, Fales HM, Yarchoan R, Tosato G. Identification of carboxypeptidase N as an enzyme responsible for C-terminal cleavage of stromal cell-derived factor-1alpha in the circulation. Blood. 2005; 105(12):4561–4568. [PubMed: 15718415]
22. Crump MP, Gong JH, Loetscher P, Rajarathnam K, Amara A, Arenzana-Seisdedos F, Virelizier JL, Baggiolini M, Sykes BD, Clark-Lewis I. Solution structure and basis for functional activity of stromal cell-derived factor-1; dissociation of CXCR4 activation from binding and inhibition of HIV-1. EMBO J. 1997; 16(23):6996–7007. [PubMed: 9384579]
23. Segers VF, Tokunou T, Higgins LJ, MacGillivray C, Gannon J, Lee RT. Local delivery of proteaseresistant stromal cell derived factor-1 for stem cell recruitment after myocardial infarction. Circulation. 2007; 116(15):1683–1692. [PubMed: 17875967]
24. Luo J, Luo Z, Zhou N, Hall JW, Huang Z. Attachment of C-terminus of SDF-1 enhances the biological activity of its N-terminal peptide. Biochem Biophys Res Commun. 1999; 264(1):42–47. [PubMed: 10527838]
25. Fiser A, Do RK, Sali A. Modeling of loops in protein structures. Protein Sci. 2000; 9(9):1753–1773. [PubMed: 11045621]
26. Davis IW, Leaver-Fay A, Chen VB, Block JN, Kapral GJ, Wang X, Murray LW, Arendall WB 3rd, Snoeyink J, Richardson JS, Richardson DC. MolProbity: all-atom contacts and structure validation for proteins and nucleic acids. Nucleic Acids Res. 2007; 35:W375–383. (Web Server issue). [PubMed: 17452350]
27. Dealwis C, Fernandez EJ, Thompson DA, Simon RJ, Siani MA, Lolis E. Crystal structure of chemically synthesized [N33A] stromal cell-derived factor 1alpha, a potent ligand for the HIV-1 “fusin” coreceptor. Proc Natl Acad Sci U S A. 1998; 95(12):6941–6946. [PubMed: 9618518]
28. Mohle R, Bautz F, Rafii S, Moore MA, Brugger W, Kanz L. The chemokine receptor CXCR-4 is expressed on CD34+ hematopoietic progenitors and leukemic cells and mediates transendothelial migration induced by stromal cell-derived factor-1. Blood. 1998; 91(12):4523–4530. [PubMed: 9616148]
29. Abbott JD, Huang Y, Liu D, Hickey R, Krause DS, Giordano FJ. Stromal cell-derived factor-1alpha plays a critical role in stem cell recruitment to the heart after myocardial infarction

but is not sufficient to induce homing in the absence of injury. Circulation. 2004; 110(21):3300–3305. [PubMed: 15533866]

30. Zhao T, Zhang D, Millard RW, Ashraf M, Wang Y. Stem cell homing and angiomyogenesis in transplanted hearts are enhanced by combined intramyocardial SDF-1alpha delivery and endogenous cytokine signaling. Am J Physiol Heart Circ Physiol. 2009; 296(4):H976–986. [PubMed: 19181961]
31. Tang J, Wang J, Yang J, Kong X. Adenovirus-mediated stromal cell-derived- factor-1alpha gene transfer induces cardiac preservation after infarction via angiogenesis of CD133+ stem cells and anti-apoptosis. Interact Cardiovasc Thorac Surg. 2008; 7(5):767–770. [PubMed: 18577527]
32. Tang J, Wang J, Yang J, Kong X, Zheng F, Guo L, Zhang L, Huang Y. Mesenchymal stem cells over-expressing SDF-1 promote angiogenesis and improve heart function in experimental myocardial infarction in rats. Eur J Cardiothorac Surg. 2009; 36(4):644–650. [PubMed: 19524448]
33. Askari AT, Unzek S, Popovic ZB, Goldman CK, Forudi F, Kiedrowski M, Rovner A, Ellis SG, Thomas JD, DiCorleto PE, Topol EJ, Penn MS. Effect of stromal-cell-derived factor 1 on stem-cell homing and tissue regeneration in ischaemic cardiomyopathy. Lancet. 2003; 362(9385):697–703. [PubMed: 12957092]
34. Kai H, Ikeda H, Yasukawa H, Kai M, Seki Y, Kuwahara F, Ueno T, Sugi K, Imaizumi T. Peripheral blood levels of matrix metalloproteases-2 and -9 are elevated in patients with acute coronary syndromes. J Am Coll Cardiol. 1998; 32(2):368–372. [PubMed: 9708462]
35. McQuibban GA, Butler GS, Gong JH, Bendall L, Power C, Clark-Lewis I, Overall CM. Matrix metalloproteinase activity inactivates the CXC chemokine stromal cell-derived factor-1. J Biol Chem. 2001; 276(47):43503–43508. [PubMed: 11571304]
36. Peng SB, Peek V, Zhai Y, Paul DC, Lou Q, Xia X, Eessalu T, Kohn W, Tang S. Akt activation, but not extracellular signal-regulated kinase activation, is required for SDF-1alpha/CXCR4-mediated migration of epitheloid carcinoma cells. Mol Cancer Res. 2005; 3(4):227–236. [PubMed: 15831676]

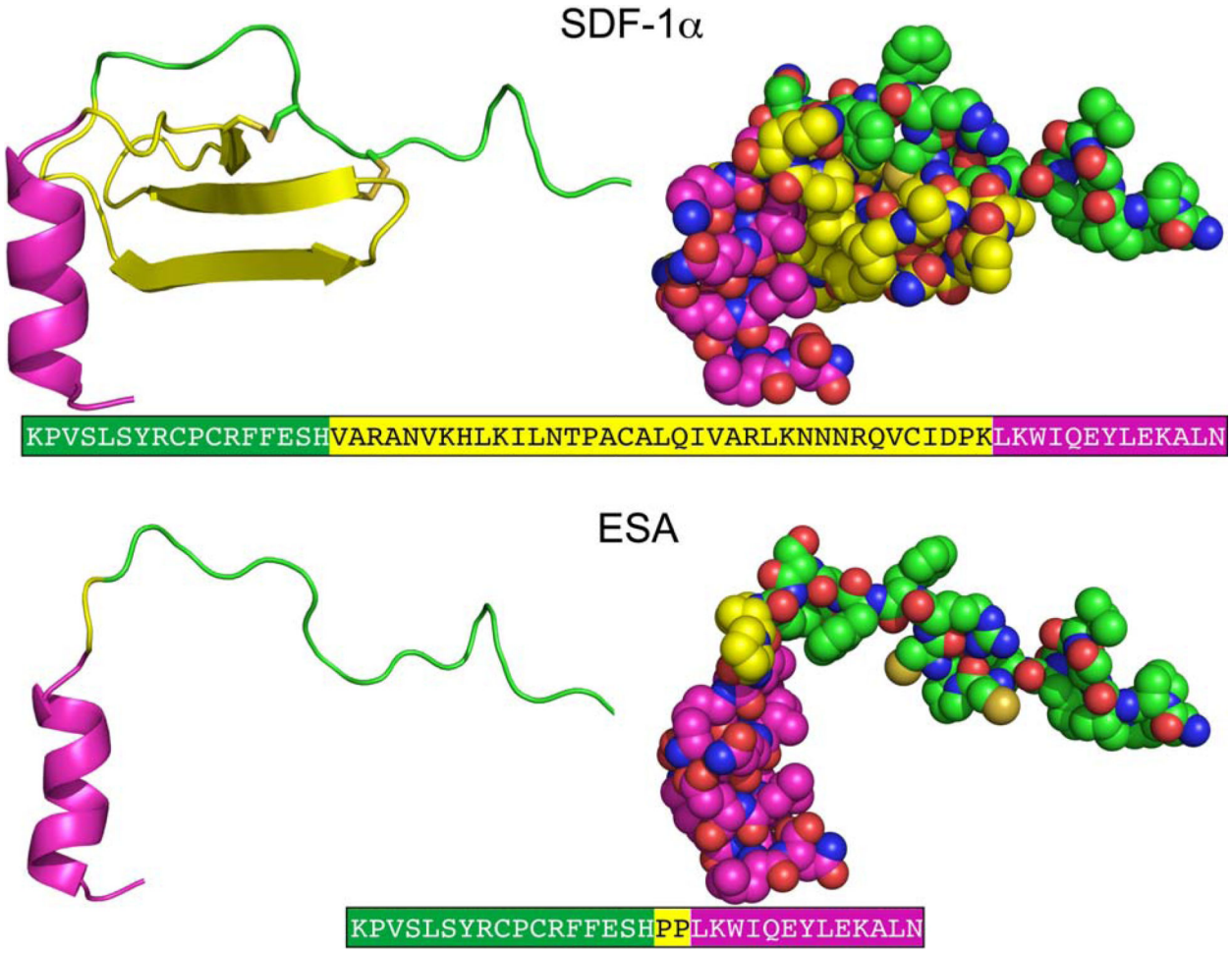

Figure 1.

Crystallographic structures of SDF[27] and designed model structure ESA. The different regions of the structure are colored as, N terminal (green), central region (yellow) and C terminal (magenta). The central β-sheet region (yellow) is replaced by a diproline linker in ESA. The corresponding amino acid sequences of SDF-1α and ESA are also depicted, where the different regions are colored accordingly.

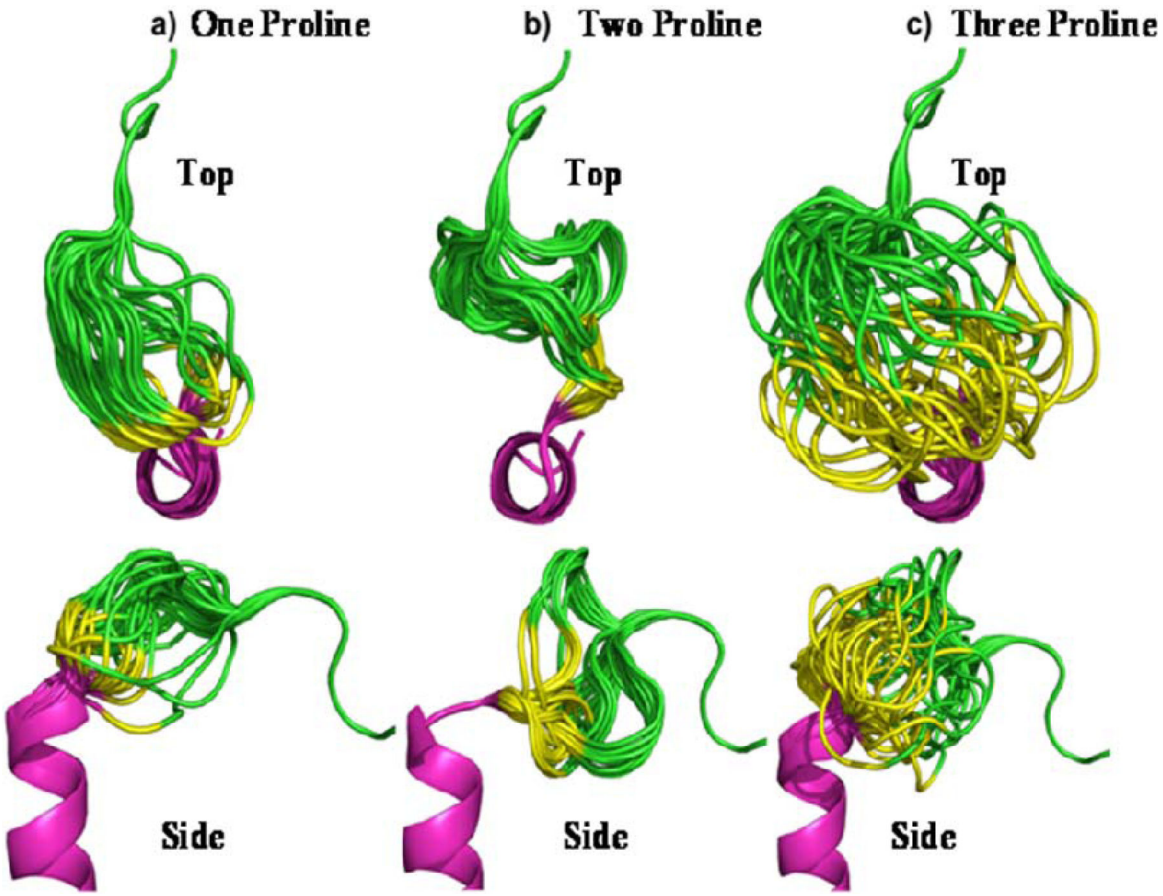

Figure 2.

Top and side view of experimental SDF analog peptides utilizing one proline (a), two proline (b), and three proline (c) residues to link the N and C terminus. The images depict a composite of the 50 most energetically stable conformations of each peptide sequence. The peptide with the two proline linker (b) adopts a more uniform tertiary profile than the others and recovers the perpendicular orientation between the N- and C- termini found in native SDF.

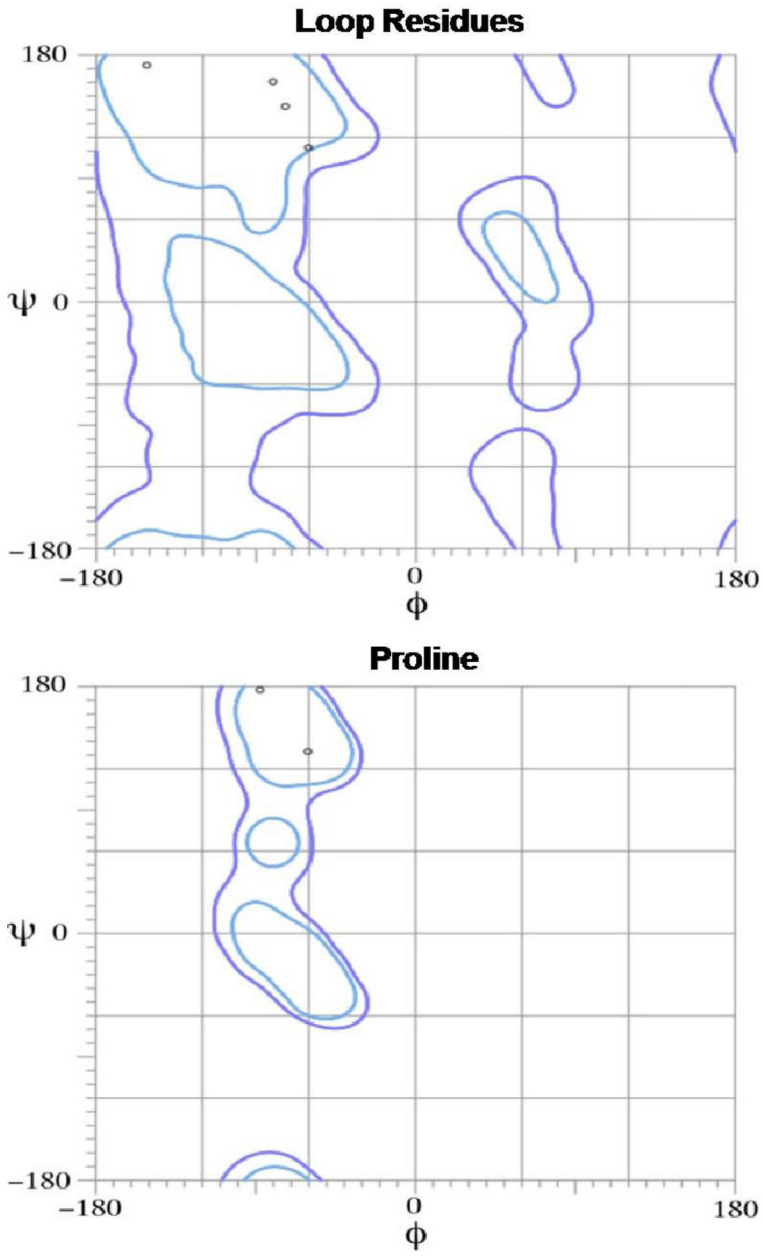

Figure 3.

All of the residues from the ESA loop or linker region are located inside favored regions in the Ramachandran plots (bounded by the blue and purple lines) indicating allowable bond angles. Most importantly, the two proline residues were found to have energetically favorable backbone dihedral angles (ϕ and ψ) consistent with those observed in natural protein structures.

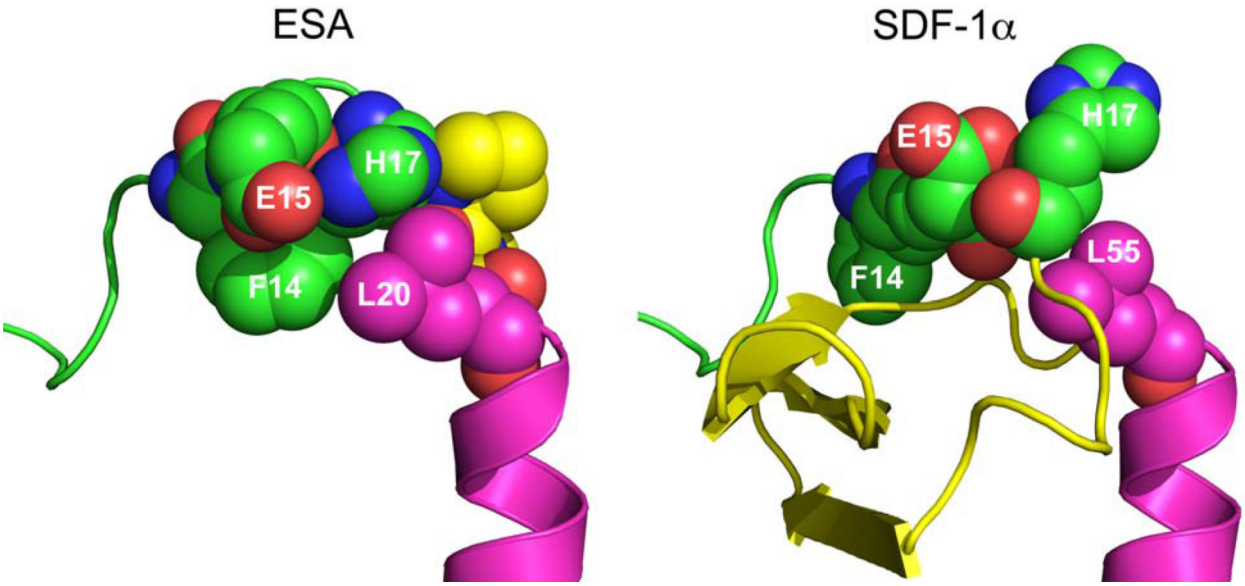

Figure 4.

Space-filling representation of the ESA and SDF-1α structures. The bulky side chain of phenylalanine 14 ($F14^{ESA}$) is interacting with glutamic acid 15 ($E15^{ESA}$), histidine 17 ($H17^{ESA}$) and to some extent with leucine 20 ($L20^{ESA}$ or residue 55 in native SDF-1α). The interactions of $F14^{SDF}$, $E15^{SDF}$, $H17^{SDF}$ and $L55^{SDF}$ are absent in crystallographic structure of SDF-1α.These new interactions form a small cluster-like structure which, when coupled with the diproline spacer (yellow in ESA), may help to provide the necessary conformational stability and rigidity found in native SDF.

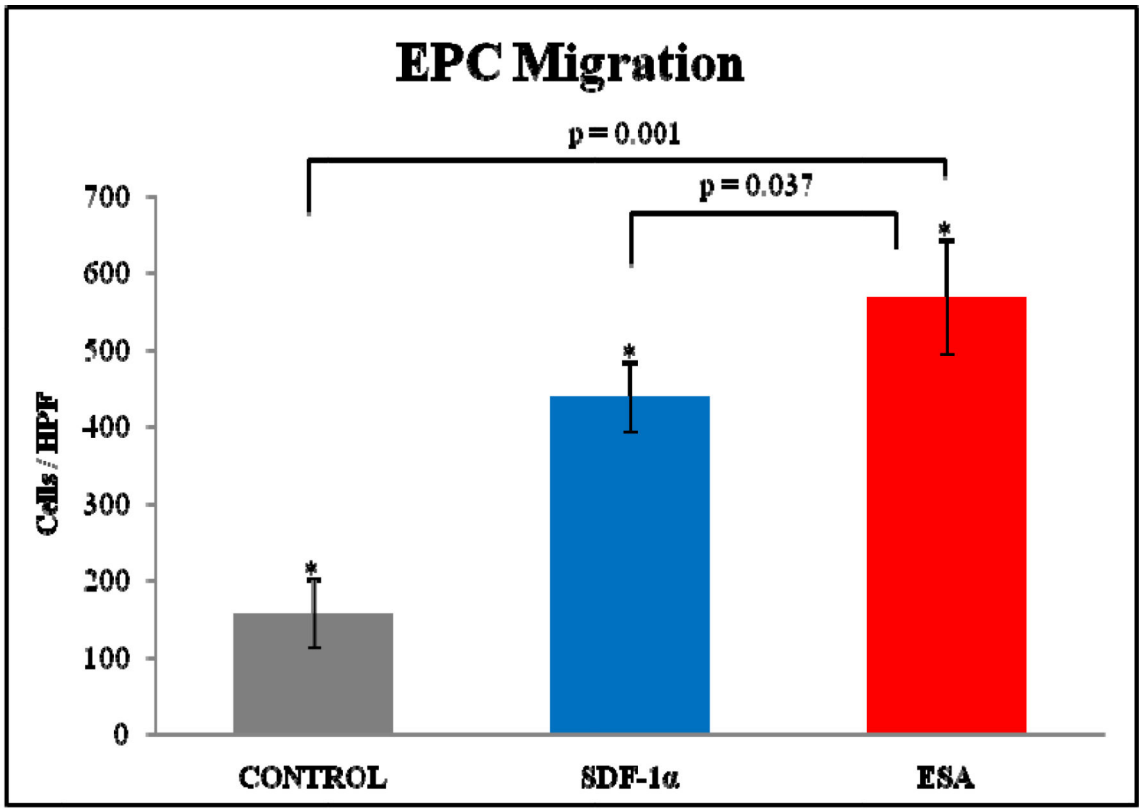

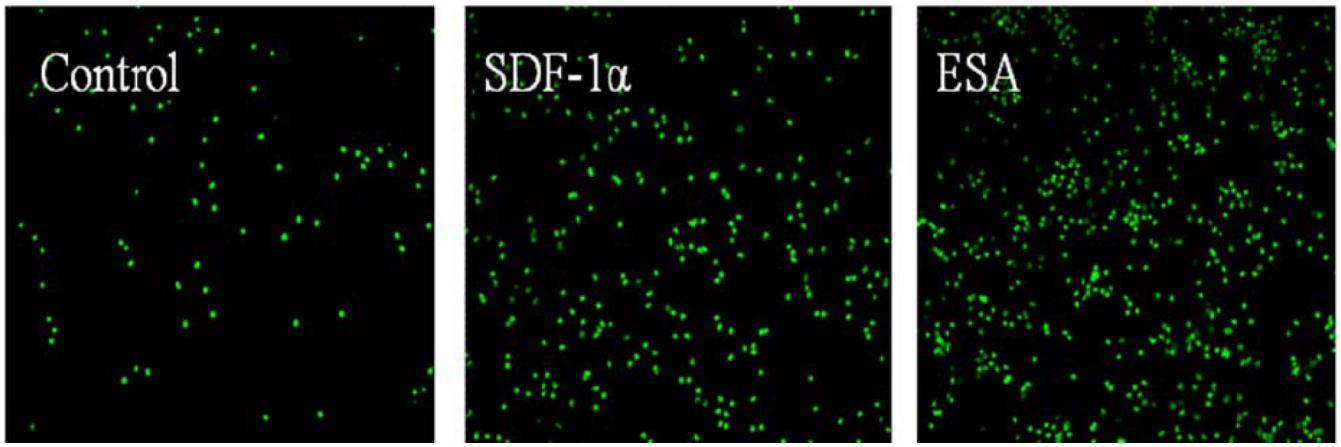

Figure 5.

Representative images of Boyden Chamber Assay filters demonstrating GFP positive EPC migration when exposed to a saline, SDF, and ESA gradient respectively.

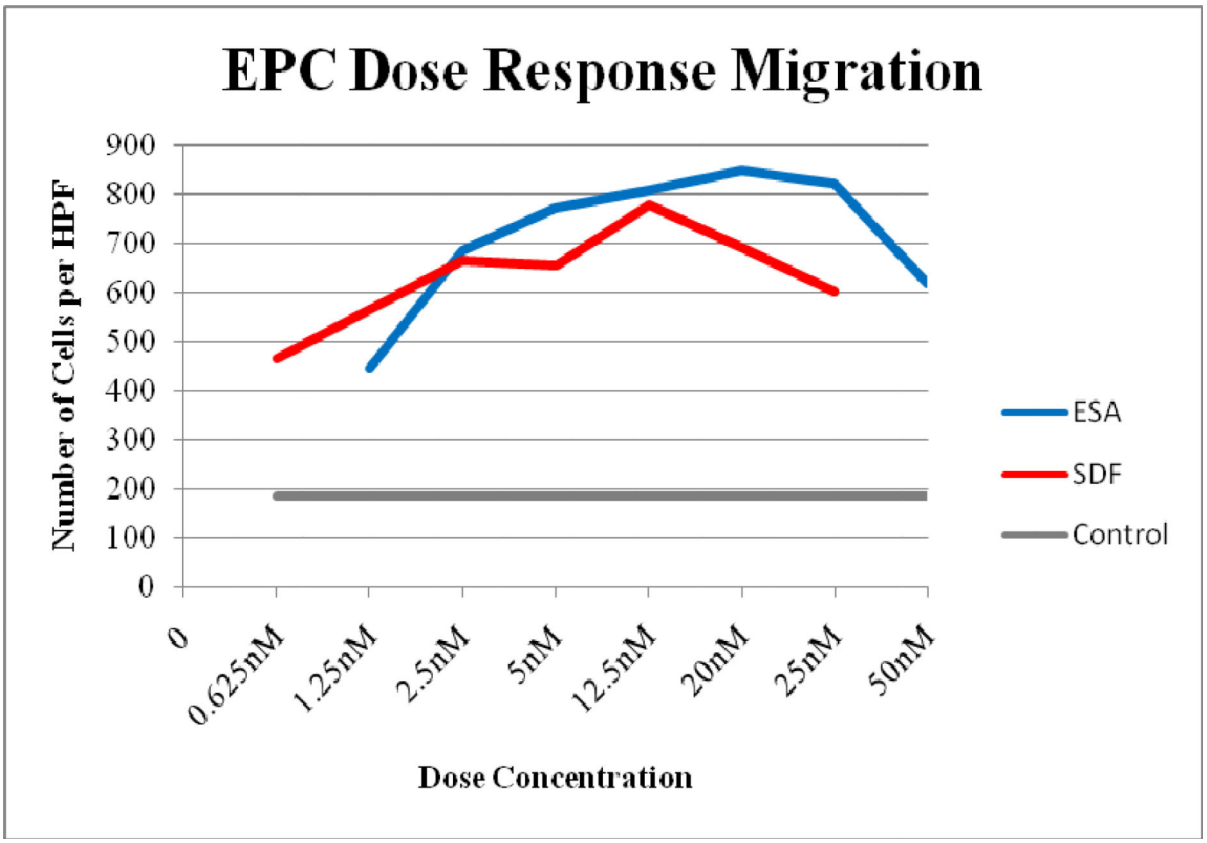

Figure 6.

Dose response curve of EPC migration comparing molar equivalent concentration gradients of ESA and SDF.

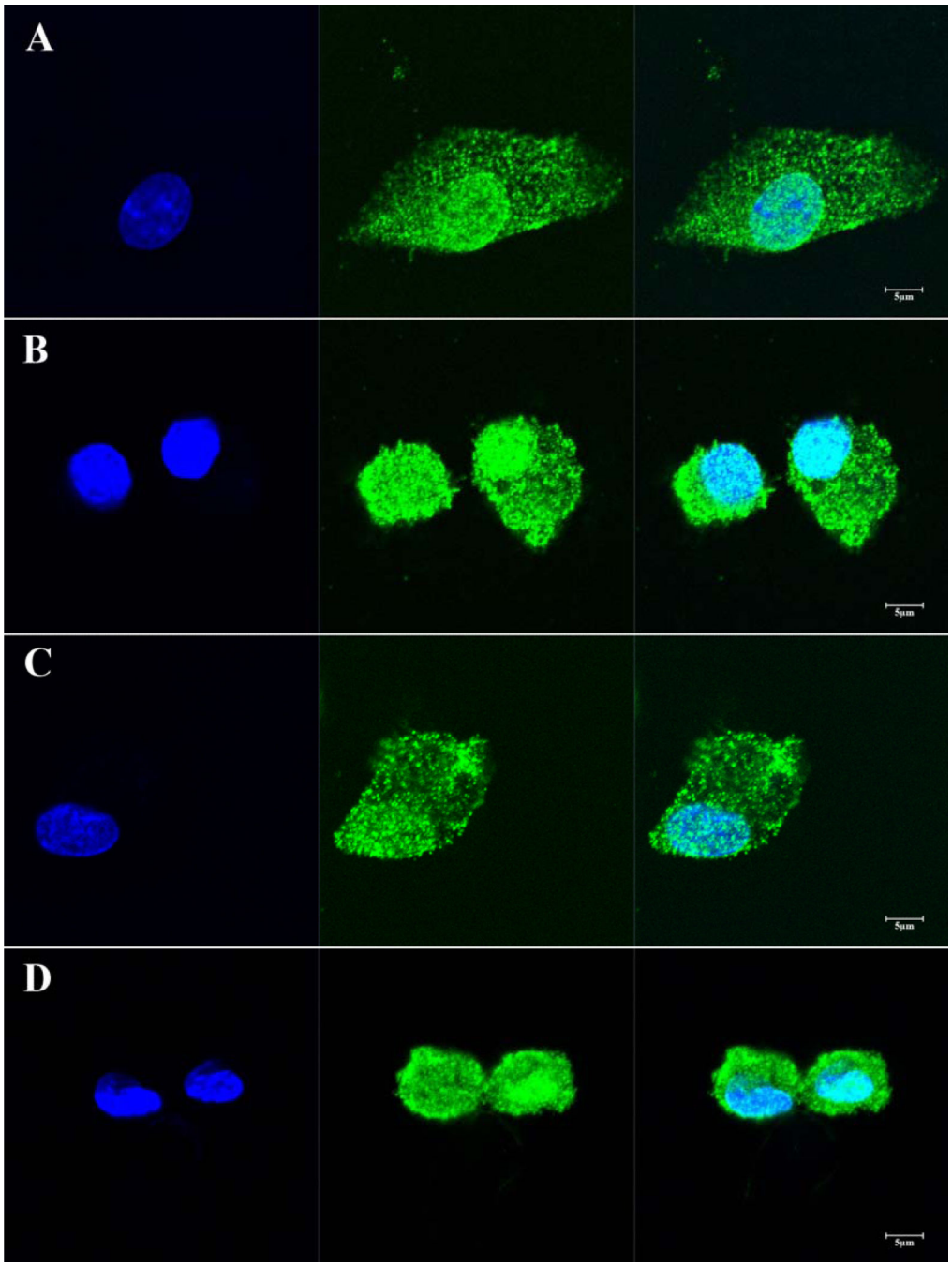

Figure 7.
Isolated EPCs cultured and stimulated with either SDF (A and B) or ESA (C and D) demonstrate robust and universal expression of the CXCR4 receptor (green). Nuclei are stained with DAPI (blue).

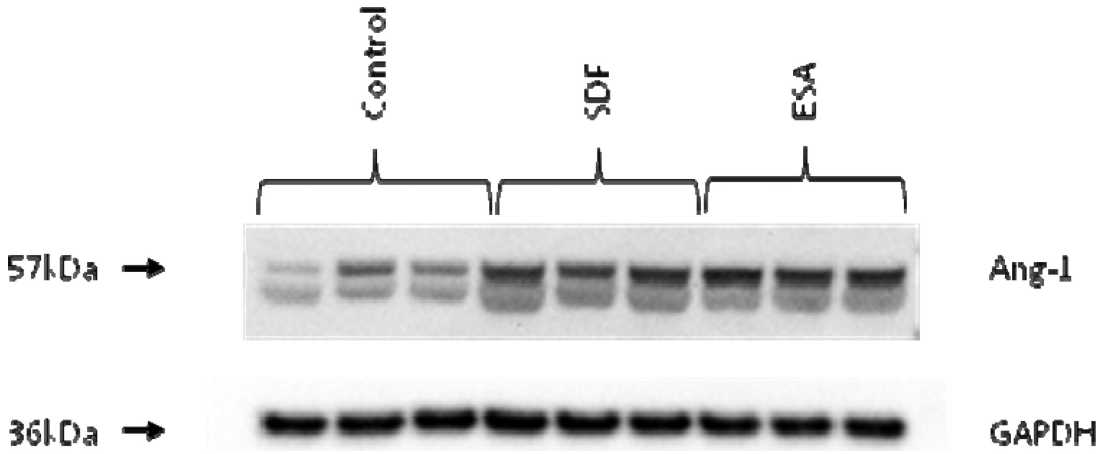

Figure 8.

At two weeks, borderzone myocardial tissue samples show increased levels of mouse Angiopoietin-1 in the ESA and SDF treated groups compared to the control group. Glyceraldehyde 3-phosphate dehydrogenase (GAPDH) staining was performed to demonstrate equivalent protein loading between lanes.

Table 1

At two weeks, ESA treated animals demonstrated improved left ventricular function by transthoracic echocardiography.

Modality	Parameter	ESA (n=10)	Control (n=7)	SDF (n=13)
Echo	Ejection Fraction (%)	57 ± 2.9	42 ± 1.6, p=0.002	51± 2.7, p=0.16
	Fractional Area Change (%)	52 ± 3.6	29 ± 4.9, p=0.001	42 ± 3.2, p=0.04
	Stroke Volume (μl)	61 ± 3.6	48 ± 2.9, p=0.02	55± 2.4, p=0.14
	Cardiac Output (ml/min)	30 ± 1.8	23 ± 1.3, p=0.01	27± 1.3, p=0.29